Excitation spectrum of bismuth donors in silicon*

N. R. Butler, P. Fisher,[†] and A. K. Ramdas

Department of Physics, Purdue University, West Lafayette, Indiana 47907

(Received 19 May 1975)

The excitation spectrum of the group-V impurity bismuth in silicon has been studied using quantitative uniaxial stress and polarized radiation in conjunction with a high-performance spectrometer and data processing system. This investigation revealed several transitions not reported previously for any donor impurity in silicon, as well as several not reported for this impurity; the energies of all these transitions agree with the calculations of Faulkner. The shear deformation potential constant Ξ_u of the Δ-conduction-band minima of silicon has been determined from the effect of uniaxial stress on the excitation spectrum of this impurity; the value of $\Xi_u = 8.70 \pm 0.18$ eV agrees very well with earlier measurements using other donor spectra. Harris and Prohofsky and Rodriguez and Schultz have developed a theory for the anomalous width of the $2p_0$ transition in this spectrum based on the interpretation by Onton et al. that this is due to a resonant interaction with an optical phonon; the shape of this transition has been carefully compared with the theory using a curve-fitting program in conjunction with the use of uniaxial stress to vary one of the parameters in the theory, the energy of the electronic state. This comparison shows that the theory is qualitatively correct when the energy of the electronic state is larger than the resonance energy, and is inadequate both for the case of electronic energy smaller than the resonance energy and for the case of the interaction with the $2p_\pm$ state.

I. INTRODUCTION

Among the group-V donors in silicon, bismuth has the largest ionization energy; its thermal ionization energy was measured[1] to be 69 meV, in contrast to 31.27 meV predicted by the recent effective-mass calculations of Faulkner.[2] The electron-spin-resonance experiments of Feher[3] established that bismuth is a substitutional impurity in silicon with a T_d site symmetry and a $1s(A_1)$ ground state. The Lyman spectrum of bismuth donors, first observed by Hrostowski and Kaiser[4] in the range 56 to 72 meV, exhibited spacings in excellent agreement with the effective-mass values for p states; the observed lines are due to $1s(A_1)$ $\rightarrow np_0, np_\pm$ transitions.[5] An ionization energy of 70.6 ± 0.3 meV was deduced by Hrostowski and Kaiser by adding the binding energy of the final np state to the observed $1s(A_1) \rightarrow np$ transition; a more recent measurement of Onton[6] yielded a value of 70.47 meV. One can thus deduce a chemical shift of ~ 39 meV for the $1s(A_1)$ ground state. In contrast, the other two sublevels of the $1s$ complex, $1s(E)$ and $1s(T_2)$, should suffer very little chemical shift. Indeed, Zeiger, Krag, and Roth[7,8] observed a doublet at 38.08 and 39.08 meV and interpreted it as a $1s(A_1) \rightarrow 1s(T_2)$ transition split by spin-orbit effects. Zwerdling, Button, and Lax[9] have studied the Zeeman effect of the $1s(A_1) \rightarrow np$ transitions; from this investigation they were able to deduce the transverse effective mass of the $\langle 100 \rangle$, i.e., the Δ-conduction-band minima and the magnetic quantum number of the final p states. Onton et al.[10] and Krag et al.[11] have reported piezospectroscopic observations on the $1s(A_1) \rightarrow np$ and the $1s(A_1) \rightarrow 1s(T_2)$ transitions, respectively. A remarkable broadening of the $1s(A_1) \rightarrow 2p_0$ transition was noticed by Onton

et al. who attributed it to a resonant interaction with a transverse optic phonon of the host lattice. Harris and Prohofsky,[12] and independently, Rodriguez and Schultz,[13] have developed a theory for this resonant interaction; we shall refer to these as HP and RS, respectively, in the rest of this paper. We have re-examined the excitation spectrum of bismuth donors in silicon under significantly improved experimental conditions[14,15] and compared the anomalous width of the $2p_0$ transition with the theoretical studies referred to above. The deformation-potential constants have also been measured for this impurity to complement the investigation of Tekippe et al.[16] (hereafter referred to as TCFR), who studied antimony, phosphorus, and arsenic impurities in silicon.

II. EXPERIMENTAL

The spectrometer used for these measurements consisted of a Perkin-Elmer model E-1 monochromator with additional source and exit optics and is described in more detail elsewhere.[15] The double-pass Ebert mount used in this monochromator exhibits an unusual stray light phenomenon, "pseudo-half-orders",[17] which was eliminated by the use of suitable filters. A polyethylene pile-of-plates polarizer was used for polarized light measurements where required. The use of a copper-doped germanium detector[18,19] gave a signal-to-noise ratio about five times better than a thermocouple detector in the region from 10 to 22 μm which includes the bismuth excitation spectrum. The infrared radiation was chopped at a frequency of 1.6 kHz, and special circuitry was used in order to obtain the highest possible performance from this detector.[15] The detector sig-

nal, processed by a lock-in amplifier,[20] was displayed on a chart recorder and simultaneously converted to digital form and punched on standard IBM cards by a special interface unit.[15] Computer processing of the data was used to increase the signal-to-noise ratio by optimum smoothing. In cases where a very high signal-to-noise ratio was required, multiple scans were averaged. A more complete description of the computer signal processing appears elsewhere.[15]

The quantitative stress cryostat used in the uniaxial stress measurements at liquid-helium temperature, as well as the details of sample preparation, are described by TCFR. A modified sample mounting procedure[15] was found to give more uniform stress than the procedure of TCFR; this involves embedding the ends of the sample in indium and the addition of a collar just above the sample in order to preserve alignment. This procedure typically gives stresses uniform to about 3% over the range from 0.5 kbar to more than 2 kbar. The sample geometry and stress apparatus limited the maximum stress to about 2 kbar.
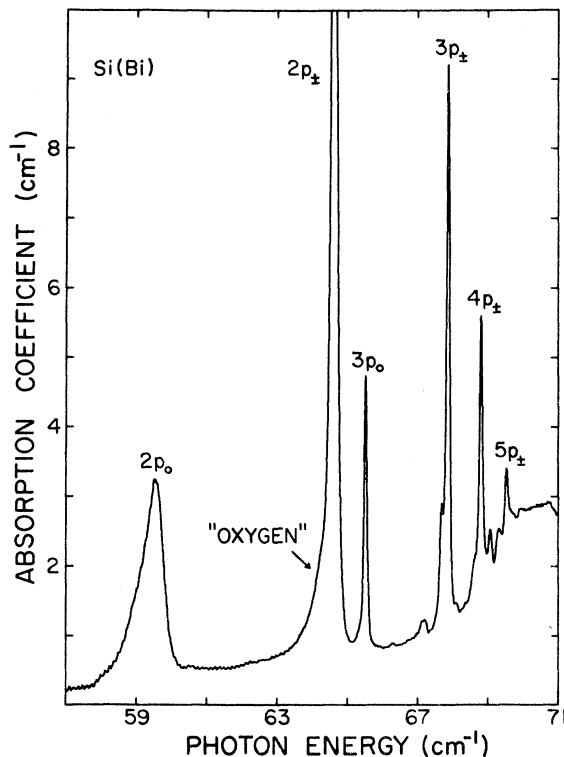

FIG. 2. Portion of the spectrum of Fig. 1 expanded to show the small lines more clearly.

FIG. 1. Excitation spectrum of bismuth donor in silicon. Liquid helium is used as a coolant. Room-temperature resistivity of this sample is about 2.5 Ω cm. The transitions shown in this figure arise from the $1s(A_1)$ ground state and are labeled with the designation of the final state. The feature labeled "oxygen" is due to the 517 cm^{-1} vibrational mode of dispersed oxygen.
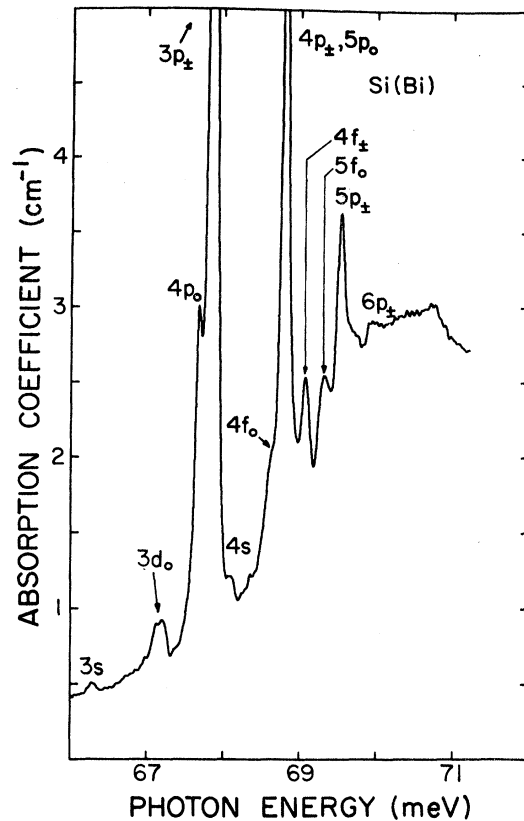
III. ZERO-STRESS SPECTRUM

The excitation spectrum of bismuth impurity in silicon is shown in Figs. 1 and 2, the latter being a portion of Fig. 1 expanded to show the smaller features more clearly. The high signal-to-noise ratio evident in these figures was obtained by averaging six scans of the spectrum. All the transitions shown arise from the $1s(A_1)$ ground state and have been labeled with the designation of the final state. Table I gives the measured line positions and a comparison of the experimental binding energies with those calculated by Faulkner.[2] The experimental binding energies have been obtained by assuming that the binding energy for the $3p_\pm$ state is correctly given by the effective-mass theory.[2] In all cases but the $2p_0$ state, the measured and calculated binding energies agree within experimental error. The case of the $2p_0$ line will be discussed later. The low-energy shoulder of the $2p_\pm$ line labelled "oxygen" is due to the 517-cm^{-1} infrared active vibrational mode of dispersed oxygen in crucible-grown silicon.[21-23] The feature in Figs. 1 and 2 at about 70.8 meV corresponds to a lattice absorption and is shown clearly in Fig. 3 for a pure-silicon sample. This feature has been ob-

TABLE I. Energies of transitions from the $1s(A_1)$ ground state of bismuth impurities in silicon and comparison of binding energies with theory. Units are in meV.

State	Transition energy (Experimental)	Binding energy (Experimental)	Binding energy (Theory[a])
$1s(A_1)$	...	70.98 ± 0.01	31.27
$2p_0$	59.54 ± 0.05	11.44 ± 0.06	11.51
$2s$	...	...	8.83
$2p_{\pm}$	64.61 ± 0.02	6.37 ± 0.03	6.40
$3p_0$	65.50 ± 0.01	5.48 ± 0.02	5.48
$3s$	66.28 ± 0.08	4.70 ± 0.09	4.75
$3d_0$	67.18 ± 0.1	3.80 ± 0.11	3.75
$4p_0$	67.68 ± 0.03	3.30 ± 0.04	3.33
$3p_{\pm}$	67.86 ± 0.01	3.12	3.12
$4s$	68.09 ± 0.08	2.89 ± 0.09	2.85
$4f_0$	68.62 ± 0.1	2.36 ± 0.11	2.33
$4p_{\pm}, 5p_0$	68.80 ± 0.01	2.18 ± 0.02	$2.19, 2.23$
$4f_{\pm}$	69.07 ± 0.03	1.91 ± 0.04	1.89
$5f_0$	69.31 ± 0.06	1.67 ± 0.07	1.62
$5p_{\pm}$	69.52 ± 0.02	1.46 ± 0.03	1.44
$6p_{\pm}$	69.90 ± 0.1	1.08 ± 0.11	1.04

[a]See Ref. 2.

served before,[24] although its shape was not as well defined as in Fig. 3. In Fig. 1, the spectral slit width ranges from about 0.3 to about 0.5 cm^{-1}; very little change in the spectrum is observed at a higher resolution.

Figures 1 and 2 clearly show all the transitions which have been reported for bismuth donors in silicon with the exception of the $1s(A_1) \rightarrow 1s(T_2)$ transition and the $2s$ transition. The energy of the transition $1s(A_1) \rightarrow 1s(T_2)$ lies outside the range of the copper-doped germanium detector. Hrostowski and Kaiser,[4] and Onton[6] have reported a $2s$ transition in this spectrum. Figure 4 shows a scan of the region where this line should appear. This figure represents the average of four scans at a
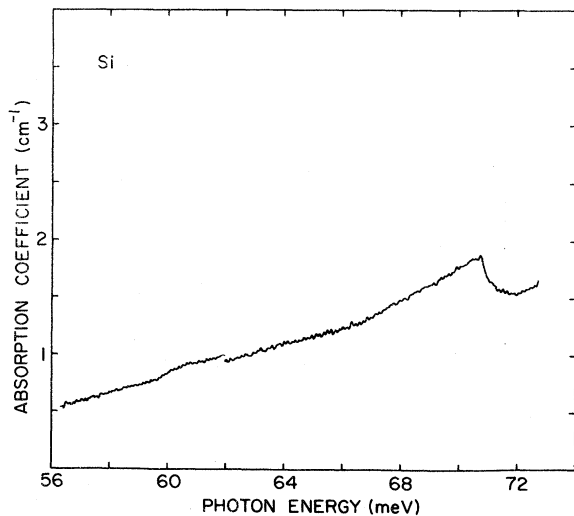
FIG. 3. Absorption spectrum of a pure-silicon sample. Liquid helium is used as a coolant. The small break in the curve is due to instrumental effects.
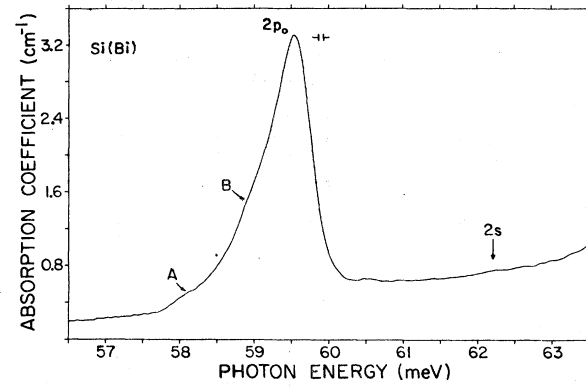
FIG. 4. $2p_0$ and $2s$ lines of bismuth in silicon recorded with high signal-to-noise ratio.

lower resolution (0.4 cm^{-1}) than that used in Fig. 1, the lower resolution being employed to improve the signal-to-noise ratio. A comparison of the peak height of the $2p_0$ with the noise in the present case and the relative heights of the reported $2s$ transition shows that the latter is either not present at all in this sample or is much smaller than reported. Hrostowski and Kaiser used a sample with about five times the concentration of the present one; it is possible that the $2s$ transition appears only at high concentrations due to the perturbing effects of other defects, as speculated by Kleiner and Krag.[25] From a comparison of Faulkner's calculations with the available line positions for a number of donors in silicon, Kleiner and Krag have identified transitions which have $2s$, $3s$, and $3d_0$ as the final states. Our spectra show excellent agreement for the $3s$ and the $3d_0$ transitions, and in addition, reveal the $4s$, $4f_0$, $4f_{\pm}$, $5f_0$, and $6p_{\pm}$ transitions. The transitions $4s$ and $4f_0$ have not been seen before for any donor in silicon. While the $5f_0$ is identified here for the first time, it was observed for phosphorous in silicon.[26] The $4f_{\pm}$ and $6p_{\pm}$ excitations, given here for the first time for bismuth impurity in silicon, were identified by Faulkner in the published spectra for lithium and phosphorus donors in silicon; these are also present in the excitation spectrum of arsenic donors.[27]

IV. EFFECT OF UNIAXIAL STRESS: DEFORMATION-POTENTIAL CONSTANT OF THE Δ-CONDUCTION-BAND MINIMA

It is well known that application of a uniaxial stress to a multivalley semiconductor results in a shift of the conduction-band minima relative to each other with, in general, a splitting of the excitation lines of the impurity spectra. TCFR have described this effect as it applies to the case of donors in silicon and have obtained the shear-deformation-potential constant of the conduction-band minima Ξ_u from the excitation spectra of Sb, As, P, and Mg donors.
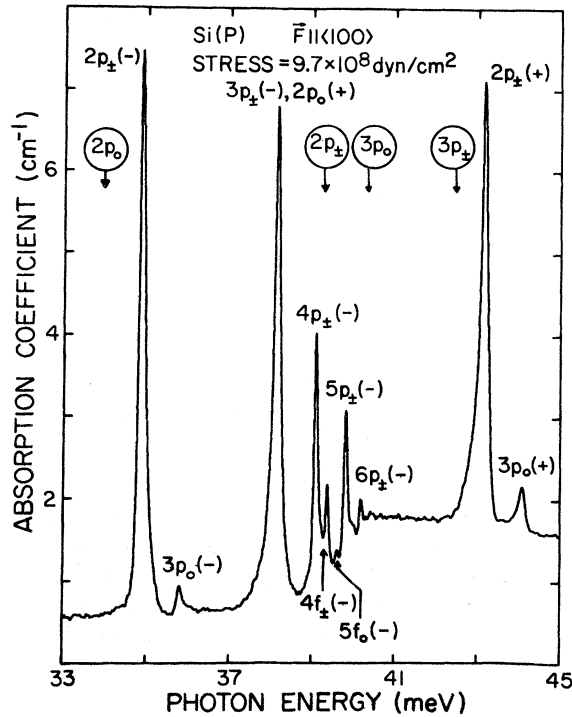
FIG. 5. Excitation spectrum of phosphorous donor in silicon with compression along a ⟨100⟩ axis. Room-temperature resistivity of this sample is about 6 Ω cm. This spectrum was recorded with a Ge(Zn) detector (see Ref. 15).

two components of a given line to its splitting. In the case of Fig. 5, this ratio is slightly over 2%. The analysis of the data follows closely that given by TCFR. The value obtained for Ξ_u by averaging the results for the different stresses (weighted according to the stress uniformity) is 8.78 ± 0.21 eV. The error is taken from the measurement with the largest stress uniformity. The error in cross sectional area is mostly due to the wedge in the sample; this has not been taken into account explicitly because it contributes to the stress nonuniformity. If the data are processed in the manner described by TCFR, the resulting value for Ξ_u is 8.78 ± 0.14 eV. Both these values are in excellent agreement with the grand average of 8.77 ± 0.07 eV given by TCFR for the four impurities studied; this demonstrates that the present technique for mounting the sample is at least as reliable as the technique described by TCFR and is probably better because it consistently gives uniform stress. The estimated error obtained from the stress uniformity should be more realistic since it attempts to take account of the uncertainty in the magnitude of the stress.

The behavior of the spectrum of bismuth donors in silicon for $\vec{F} \parallel \langle 100 \rangle$ is given in Fig. 6; this spectrum has a stress uniformity of 2.6%. Figure 7 is a plot of the splitting of the $2p_\pm$ line as a function of applied stress. The linearity of this splitting is shown by the solid line corresponding to a linear
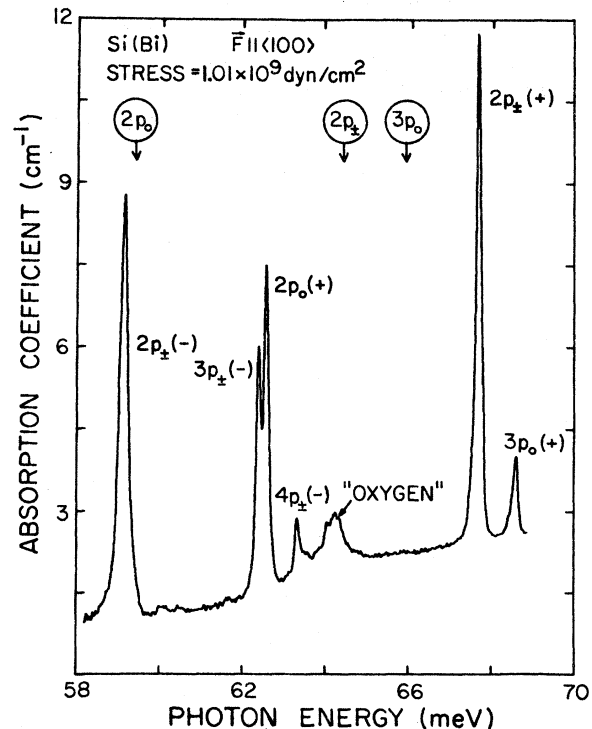
In order to test the new sample mounting procedure used in this investigation, Ξ_u was remeasured with a phosphorous-doped silicon sample. For reasons discussed by TCFR, the determination of Ξ_u is most precise when the force is applied along a ⟨100⟩ direction. A typical spectrum, recorded without a polarizer, for a compressive force $\vec{F}$ parallel to a ⟨100⟩ crystallographic direction is shown in Fig. 5. It might be noted that apart from the coincidence of the $2p_0(+)$ component with the $3p_\pm(-)$ component, the spectrum comprised of all the lower-energy components is identical to the zero-stress spectrum but shifted to lower energy. This is an excellent demonstration of the fact that all the p-like states are characterized by the same Ξ_u. The measurement does not extend to sufficiently low energy to include the $2p_0(-)$ component. The sharpness of the lines in this figure indicates the quality of the stress uniformity achievable with the stress cryostat using the improved sample mounting procedure. The part of the linewidth due to nonuniformity in the stress is governed by the slope of the line position versus stress curve. It is the stress nonuniformity which in practice limits the precision with which the value of Ξ_u can be obtained. The relative nonuniformity can be estimated from the ratio of the average width of the

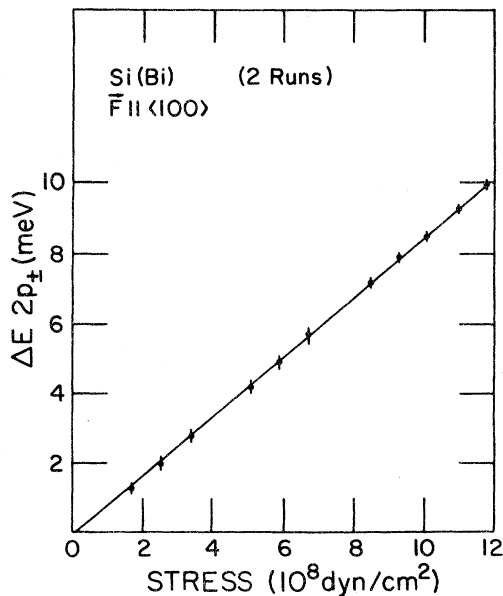FIG. 6. Excitation spectrum of bismuth donor in silicon with compression along a ⟨100⟩ axis.

FIG. 7. Splitting of the $2p_{\pm}$ state as a function of stress for bismuth donor in silicon.

least-squares fit to the data; the vertical bars represent the average of the half widths of the two components. Proceeding as for phosphorous above, Ξ_u was computed to be 8.70 ± 0.18 eV for the average of the weighted average of two runs and 8.81 ± 0.17 eV using the technique of TCFR.

It is well known that the $1s(A_1)$ state exhibits a nonlinear shift with uniaxial stress. This shift can be determined, following TCFR, from the deviation from linear stress dependence of the $2p_{\pm}(+)$ and the $2p_{\pm}(-)$ components; the data points in Fig. 8 were obtained following this procedure. The solid line gives the shift calculated using Eq. (10) of TCFR (see also Wilson and Feher[28]) which incorporates the singlet-doublet spacing $6\Delta_c$ and Ξ_u as parameters. The value of $6\Delta_c$ for bismuth has not been determined experimentally but it should be somewhat larger than 39 meV, the singlet-triplet spacing determined by Krag et al.[11] and should be close to the difference between the experimental and effective-mass ground-state energies (see Table I); this latter difference is ~ 39.7 meV. For these reasons we chose $6\Delta_c = 40$ meV and $\Xi_u = 8.8$ eV to compute the solid line. A fit with the experimental results can be obtained only for $6\Delta_c \approx 65$ meV if the Ξ_u of the excited state is to be retained. The dashed curve corresponds to $6\Delta_c = 40$ meV but $\Xi_u = 6.8$ eV. This value of the ground-state deformation-potential constant is smaller than those obtained for the other group-V donors and follows the trend already indicated that the ground-state deformation-potential constant decreases with increasing ground-state binding energy.

V. ANOMALOUS BROADENING OF THE $2p_0$ TRANSITION

A. Experimental results

The anomalous broadening previously reported for the $2p_0$ line is clearly shown in Figs. 1 and 4; the width of this line, about eight times that of the other prominent lines, has been interpreted as due to an interaction between the donor electron and optical phonons of the energy of the $2p_0$ transition.[10] This interpretation was tested by observing the behavior of the stress-induced components of this line as a function of their energies. In the present investigation, the results of which are given below, the anomalous broadening has been examined in considerably more detail.

Figure 9 shows the two components of the $2p_0$ line for compression along [110] with radiation propagating along $\vec{k} \parallel [1\bar{1}1]$ but without a polarizer. Note that the $2p_0(-)$ component, although still broad, is now almost symmetric, while the $2p_0(+)$ component is much sharper than the zero-stress line of Fig. 4. The small fluctuations in the signal are the remnants after smoothing of interference fringes from the transmission filter. Figure 10 shows the $2p_0(-)$ component for three different values of stress chosen to demonstrate that the asymmetry is reversed for components on opposite sides of the energy for which the component exhibits a maximum width; we define this energy as
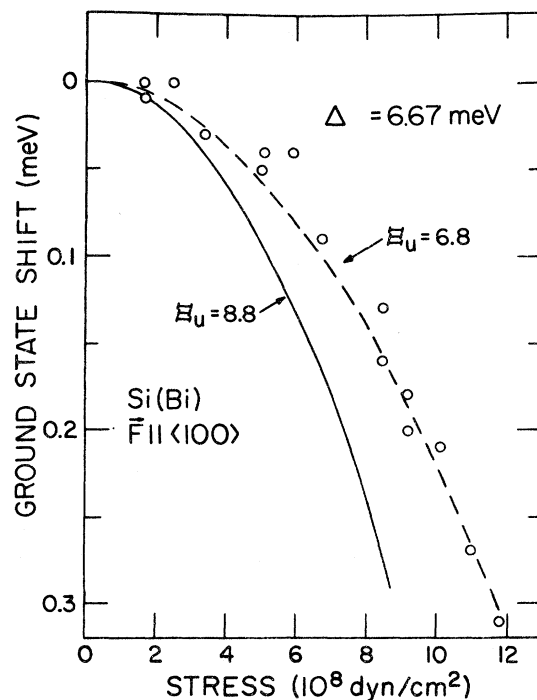

FIG. 8. Shift of the $1s(A_1)$ ground state of bismuth donor in silicon as a function of stress. (See TCFR for procedure.)
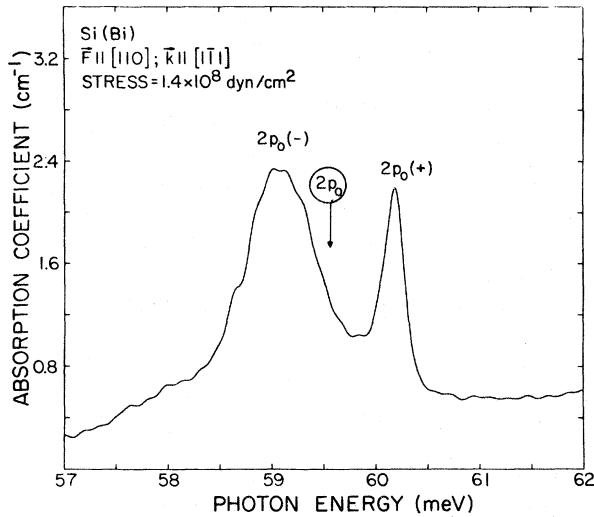
FIG. 9. Splitting of the $2p_0$ line with compression along a $\langle 110 \rangle$ axis.

the resonance energy. The higher-energy component evident in Fig. 9 has been eliminated by the use of radiation polarized parallel to the direction of $\vec{F}$.[29] This same type of effect is also seen for $\vec{E} \parallel \vec{F} \parallel [100]$, where again only the low-energy component is present. In this case, the low-energy component can be shifted by four times as much for a given stress as for $\vec{F} \parallel [110]$, and thus the component can be followed over a much larger range of energies.[16] Some results for this orientation are shown in Fig. 11. For this direction of
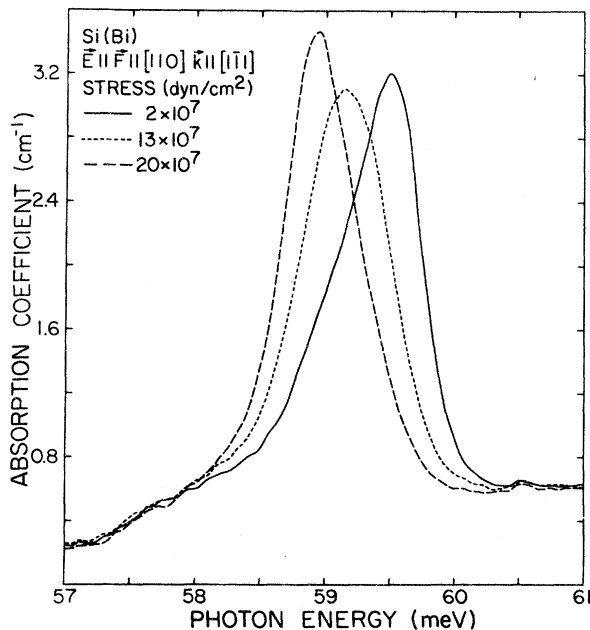

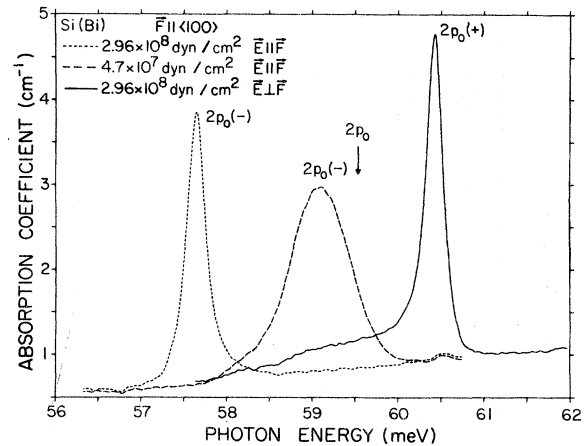FIG. 10. $2p_0(-)$ component undergoing resonance.

FIG. 11. Typical appearance of the two components of the $2p_0$ line at different stresses.

compression, the two components of $2p_0$ have opposite polarization and thus can be observed separately. As the stress is increased from zero to the maximum value shown in Fig. 11, the high-energy component sharpens and slowly develops the broad low-energy tail seen in the figure. The low-energy component achieves a symmetric shape at a stress of 4.7×10^7 dyn/cm^2; as the stress is increased further, $2p_0(-)$ becomes slightly asymmetric and sharpens, and then continues to sharpen and become almost symmetric as is seen for the larger stress of Fig. 11. It should be noted that the low-energy component does not develop a broad tail of the type exhibited by the high-energy component. It is found that for compression along both $\langle 100 \rangle$ and $\langle 110 \rangle$ the low-energy component assumes an almost symmetrical shape and maximum width of 0.85 meV at an energy of ~ 59.1 meV, as is seen in Figs. 10 and 11.

B. Comparison with theory

The shape of an impurity absorption line in the presence of an electron-phonon interaction has been given in the theories of HP and RS. In HP's theory, the impurity electron is coupled to one phonon mode which then decays into the thermal background with a lifetime of Γ_λ. The absorption obtained by them for such a coupled state has the form

$$P(\omega) \propto \mathrm{Im} \; \frac{\hbar\omega - \hbar\omega_L - \frac{1}{2} i\Gamma_\lambda}{(\hbar\omega - \hbar\omega_I - \frac{1}{2} i\Gamma_\gamma)(\hbar\omega - \hbar\omega_L - \frac{1}{2} i\Gamma_\lambda) - \beta^2} .$$

$$(1)$$

Here ω is the photon angular frequency, $\hbar\omega_L$ the energy of the phonon to which the electron state is coupled, $\hbar\omega_I$ is the energy of the electronic state in the absence of coupling, Γ_γ is the natural width of the uncoupled impurity state, and β is the coupling constant between the electron and the phonon. The RS theory takes into account the interaction
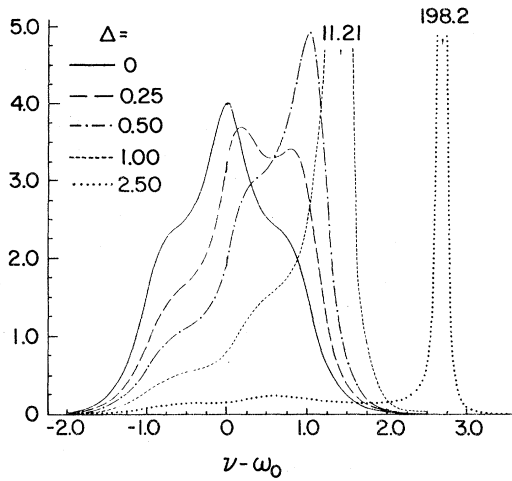
FIG. 12. Calculated line shapes [see Ref. 13, Fig. 5(c)].

of the electron with all phonons. It is shown that the significant interaction is with the transverse optical phonons with wave vectors approximately in the $\langle 110 \rangle$ direction. RS demonstrate that their theory includes the result given by HP as a special case. Figure 12 shows some of the results calculated by RS. The shape of the $2p_0$ line in Fig. 4 is similar to that of Fig. 12 for $\Delta = 0.50$, where $\Delta \equiv \epsilon - \hbar\omega_0$. Here ϵ is the energy of the $2p_0$ state and corresponds to $\hbar\omega_I$, while ω_0 is the resonant frequency for the electron-phonon interaction and corresponds to ω_L. The two features labelled A and B in Fig. 4 might correspond to the two low-energy undulations in RS's results, although the latter are more prominent. The shape of $2p_0(+)$ in Fig. 11 is also similar to that in Fig. 12 for $\Delta = 2.50$ in that it shows a tail extending to lower energies. However, the "in-resonance" $2p_0(-)$ components of Figs. 10 and 11 do not exhibit the two symmetric wings shown for $\Delta = 0$ in Fig. 12, nor is the shape of its peak the same as that of the latter. In addition, the theory predicts that as the $2p_0(-)$ component moves through the resonant position to lower energies, its shape should be mirrored about the resonant energy; this is not so, as may be seen from Fig. 11.

In order to make a quantitative analysis, we have employed a curve-fitting procedure for the line shapes of the two components of $2p_0$ for different values of stress.[15] The HP function [Eq. (1)], rather than the more complex expression of RS, was used in this analysis for both the $2p_0(+)$ and $2p_0(-)$ components. The parameters in Eq. (1) are determined from the experimental results as follows. An error function is defined which characterizes the discrepancy between the theoretical form and the experimental data. The parameter

values which minimize the value of this function are then found by an iterative procedure. The error function used here is chosen so that if all the errors are due to random noise from the detector, the resulting parameter values are those which have the highest probability of being correct. The method used for finding the parameter values from the data and the theoretical form of the line shape is called a modified-Gauss method, and is similar to one described by Bard.[30]

The success of the fit for the $2p_0(+)$ component is illustrated in Fig. 13. In making this fit, Γ_γ was set equal to 0.1 meV; this is the width of the $3p_0$ line (see Fig. 1) whose final state should be most similar to that of the $2p_0$ transition. If the curve-fitting program is allowed to treat Γ_γ as an adustable parameter, a better fit is achieved, but the values of Γ_γ obtained are always negative. This implies that the HP function does not fit the data as well as that function obtained by changing the sign of Γ_γ in the HP expression, but this new function obviously does not have physical meaning since it can become negative. A similar fit was attempted for the $2p_0(-)$ component, but the results were unsatisfactory, implying that the HP function is not appropriate in this case. For this reason, the low-energy $2p_0$ components were fitted with two types of simple asymmetric functions, viz. dual-width Lorentzians or Gaussians. By dual width is meant that for energies above the peak position the function has one width, while for energies below another width was used. The better fit was obtained using the Lorentzian; this is illustrated in Fig. 14. The energy of the impurity state was estimated from the center of gravity of the component. A means for doing this with the Lorentzian fit was
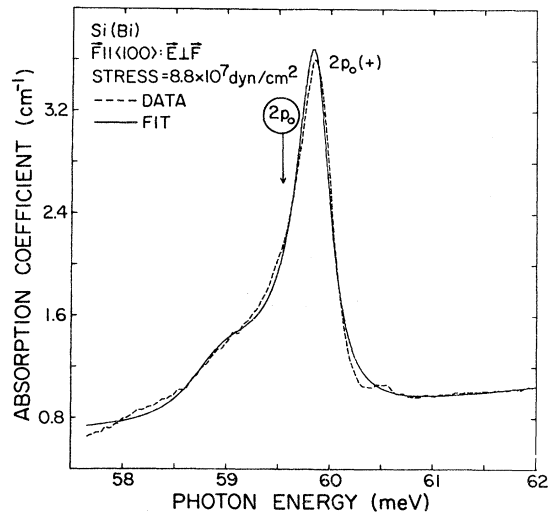

FIG. 13. Results of curve fitting to the $2p_0(+)$ component using the function given in Ref. 12.
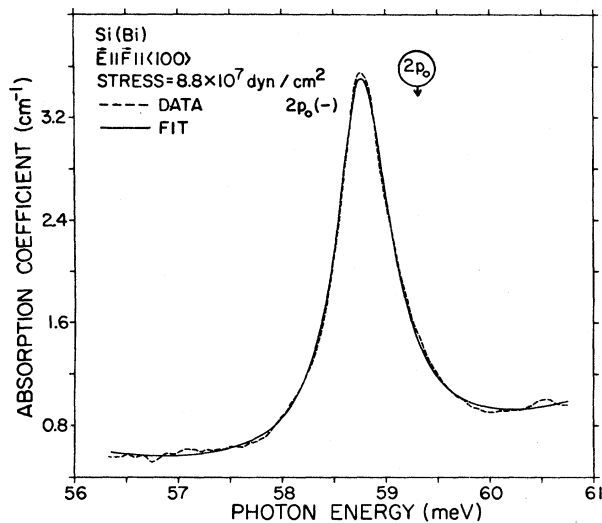
FIG. 14. Results of curve fitting to the $2p_0(-)$ component using a dual-width Lorentzian.

not discovered, and thus the asymmetric Gaussian was used to determine the center of gravity. This is not an unreasonable approach, since both procedures are somewhat arbitrary and give similar results.

Some results of the above analyses for $\vec{F} \parallel \langle 100 \rangle$ are shown in Fig. 15. The upper curve, with data points designated by plus signs, is a plot of the peak position of the $2p_0(+)$ component as a function of stress. A similar plot for the $2p_0(-)$ component is defined by the encircled data points. The values of $\hbar\omega_I$ obtained from the HP fits for $2p_0(+)$ are given by the crosses; the line drawn through these represents the results of a linear least-squares fit to them. The values of $\hbar\omega_L$ obtained from the same fits are indicated by the triangular symbols. The plot of the centers of gravity of the $2p_0(-)$ components is depicted by the square symbols and the straight line a drawn through these points, and is the result of a linear least-squares fit.

The two straight lines labeled $\hbar\omega_I$ and a in Fig. 15 can be used to determine Ξ_u. This is found to be 8.8 eV, which is in remarkable agreement with that given in Sec. IV. In making this estimate, the shift of the ground state was ignored. However, even for the maximum stress of 3×10^8 dyn/cm^2 in Fig. 15, the ground state experiences very little shift, as may be verified from Fig. 8. The intercepts of the fits to $\hbar\omega_I$ and a are almost identical and predict an uncoupled transition energy for the $2p_0$ line of 59.33 meV, which agrees well with the values of 59.34 meV obtained for $\hbar\omega_I$ by a curve fitting of the zero-stress line of Fig. 4. This leads to a binding energy for the $2p_0$ state of 11.65 meV, which though not unreasonable is not in as good

agreement with the calculated value (see Table I) as that obtained from the peak position of the zero-stress $2p_0$ line.

Under the conditions of HP's calculation, the value of $\hbar\omega_L$ obtained should be independent of the energy of the impurity state. Raman studies[31] have demonstrated that the zone-center phonon in silicon exhibits insignificant changes in energy at the stresses of Fig. 15. However, the two-phonon studies of Hobson and Paige[32] suggest that the off-center phonons may have larger deformation-potential constants than those at the center. In view of the manner in which $\hbar\omega_L$ has been obtained in the present investigation, its change with stress, shown in Fig. 15, is not significant. The average value of $\hbar\omega_L$, including the zero-stress value, is 59.2 meV, which agrees well with the resonance energy of ~ 59.2 meV estimated from the position of the $2p_0(-)$ component when it exhibits its maximum width. The width Γ_- of the $2p_0(-)$ component as a function of stress is also shown in Fig. 15 and is designated by the inverted triangles; these values are those given by the half-width of the dual-width-Lorentzian fit described above.

The results portrayed in Fig. 15 clearly show that the electron-phonon interaction is stronger
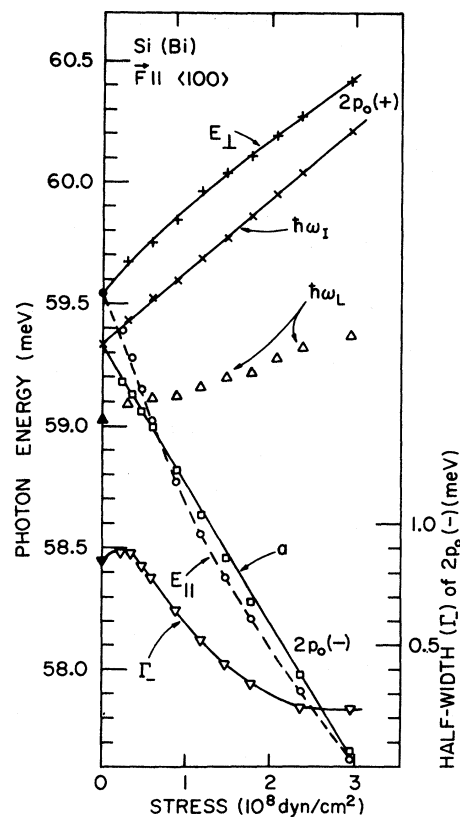

FIG. 15. Plot of various parameters for both components of the $2p_0$ line as a function of stress.
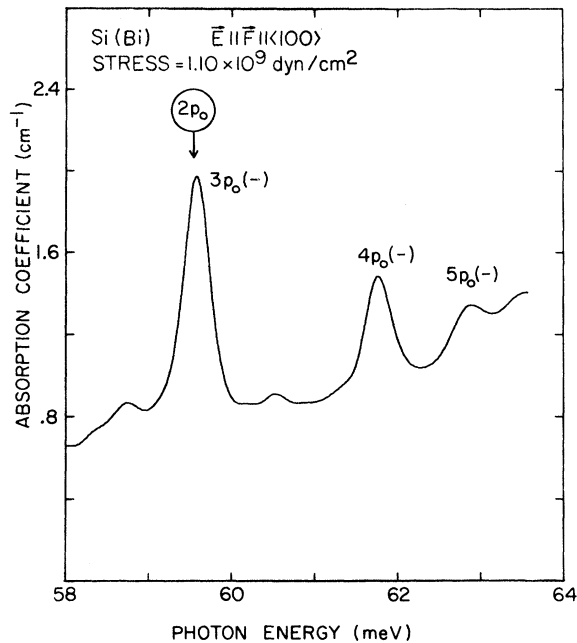
FIG. 16. $3p_0(-)$ component at the resonance energy of the $2p_0$ line.

broadening would occur for these two excitations. Figure 16 shows the $3p_0(-)$ component at the zero-stress energy of the $2p_0$ line. The half-width of this component is ~ 0.35 meV, which is $2\frac{1}{2}$ times narrower than the zero-stress $2p_0$ line while no asymmetric effects are evident. There is no indication that the half-width is due to anything other than stress nonuniformity. A calculation[34] of the ratio of the strengths of the electron-phonon interaction of the $3p$ and $2p$ states shows that it is ~ 0.04; hence, the lack of observable resonance is not unexpected. The spectrum of Fig. 6 shows the $2p_\pm(-)$ component shifted to the $2p_0$ resonance energy. The half-width of this component is ~ 0.2 meV and can also be attributed to stress nonuniformity. In order to compare the electron-phonon interaction effects for $2p_0$ and $2p_\pm$, it is necessary to take into account the anisotropy of the effective mass of the donor electron; neither RS nor HP have incorporated this into their theory.

D. Conclusions

The comparison between the experimental line shape and the theory for resonant electron-phonon interactions can be summarized as follows: (i) The theories of HP and RS both give qualitatively correct results for the shape of the $2p_0(+)$ component, but neither gives the observed line shape to within experimental error. (ii) Neither theory predicts the smaller interaction for the $2p_0(-)$ component, although the results of RS could perhaps be extended to account for this by considering the next term in their expansion for phonon energy. In the absence of even an approximate theory, we have used arbitrary functions to analyze the shape of this component. (iii) The RS theory predicts the same interaction for the $2p_\pm$ component as for the $2p_0$ (the HP theory makes no prediction about the relative interaction), but the experimental results show that the interaction is at least five times stronger for the $2p_0$. (iv) A calculation in the framework of the RS theory correctly predicts that the interaction is much smaller for the $3p_0$ line than for the $2p_0$.

ACKNOWLEDGMENTS

for electron energies above the resonance energy than for those below, since the observed peak positions for $2p_0(+)$ are substantially different from the corresponding $\hbar\omega_I$ values. At the maximum stress of 3×10^8 dyn/cm², the $2p_0(-)$ component shows no discernible interaction, whereas the coupling is still significant for the $2p_0(+)$ component even though the two components are separated from the resonance energy by about the same amount. This, as already mentioned, is not in agreement with the theory. The unsymmetric behavior around the resonance might be accounted for in the framework of the RS calculation if the gradient of the phonon dispersion is zero at $\hbar\omega_L$, as is suggested from the neutron-scattering data.[33] This would require the inclusion of the next term in the expansion used by RS for the phonon energy, which in turn might give rise to the observed asymmetry.

C. The $3p_0$ and $2p_\pm$ lines

It is possible to apply sufficient stress to move both the $3p_0(-)$ and $2p_\pm(-)$ components to near the resonant position of the $2p_0$ line. It might be expected that under these conditions an anomalous

[1]F. J. Morin quoted in H. J. Hrostowski and R. H. Kaiser, J. Phys. Chem. Solids 4, 315 (1958).
[2]R. A. Faulkner, Phys. Rev. 184, 713 (1969). See also W. Kohn, *Solid State Physics*, edited by F. Seitz and D. Turnbull (Academic, New York, 1957), Vol. 5,

p. 257.

[3]G. Feher, Phys. Rev. 114, 1219 (1959).

[4]H. J. Hrostowski and R. H. Kaiser, J. Phys. Chem. Solids 4, 315 (1958).

[5]For a general review and the nomenclature prevalent in this field, see P. Fisher and A. K. Ramdas, *Physics of the Solid State*, edited by S. Balakrishna, M. Krishnamurthi, and B. Ramachandra Rao (Academic, New York, 1969), p. 149.

[6]A. Onton, Ph. D. thesis (Purdue University, 1967) (unpublished).

[7]H. J. Zeiger, W. L. Krag, and L. M. Roth, MIT Lincoln Laboratory, Quarterly Report, Solid State Research, 1961 (unpublished).

[8]L. M. Roth, MIT Lincoln Laboratory, Solid State Research Report No. 3, 1962 (unpublished).

[9]S. Zwerdling, K. J. Button, and B. Lax, Phys. Rev. 118, 975 (1960).

[10]A. Onton, P. Fisher, and A. K. Ramdas, Phys. Rev. Lett. 19, 781 (1967).

[11]W. E. Krag, W. H. Kleiner, and H. J. Zeiger, *Proceedings of the Tenth International Conference on the Physics of Semiconductors, Cambridge, Massachusetts,* 1970, edited by S. P. Keller, J. C. Hensel, and F. Stern (U. S. A. E. C., Division of Technical Information, Washington, D. C., 1970), p. 271.

[12]S. M. Harris and E. W. Prohofsky, Phys. Rev. 170, 749 (1968).

[13]S. Rodriguez and T. D. Schultz, Phys. Rev. 178, 1252 (1969).

[14]A preliminary report was made in N. R. Butler, P. Fisher, and A. K. Ramdas, Bull. Am. Phys. Soc. 18, 91 (1973).

[15]N. R. Butler, Ph. D. thesis (Purdue University, 1974) (unpublished).

[16]V. J. Tekippe, H. R. Chandrasekhar, P. Fisher, and

A. K. Ramdas, Phys. Rev. B 6, 2348 (1972).

[17]N. R. Butler, Appl. Opt. 9, 1475 (1970).

[18]Manufactured by Texas Instruments, Dallas, Tex.

[19]N. R. Butler and P. Fisher, Phys. Lett. A 47, 391 (1974).

[20]Type HR-8, manufactured by Princeton Applied Research, Princeton, N. J.

[21]H. J. Hrostowski and R. H. Kaiser, Phys. Rev. 107, 966 (1957).

[22]H. J. Hrostowski and B. J. Alder, J. Chem. Phys. 33, 980 (1960).

[23]D. R. Bosomworth, W. Hayes, A. R. L. Spray, and G. D. Watkins, Proc. R. Soc. Lond. A 317, 133 (1970).

[24]F. A. Johnson, Proc. Phys. Soc. Lond. 73, 265 (1959).

[25]W. H. Kleiner and W. E. Krag, Phys. Rev. Lett. 25, 1490 (1970).

[26]Unpublished results of R. L. Aggarwal and A. K. Ramdas, quoted in L. T. Ho and A. K. Ramdas, Phys. Rev. B 5, 462 (1972), Fig. 2.

[27]Unpublished results of R. L. Aggarwal and A. K. Ramdas, quoted in Ref. 5.

[28]D. K. Wilson and G. Feher, Phys. Rev. 124, 1068 (1961).

[29]R. L. Aggarwal and A. K. Ramdas, Phys. Rev. 137, A602 (1965).

[30]Y. Bard, SIAM J. Numer. Anal. 7, 157 (1970).

[31]E. Anastassakis, A. Pinczuk, E. Burstein, F. H. Pollak, and M. Cardona, Solid State Commun. 8, 133 (1970).

[32]G. S. Hobson and E. G. S. Paige, Proc. Phys. Soc. Lond. 88, 437 (1966).

[33]G. Dolling, *Inelastic Scattering of Neutrons in Solids and Liquids* (International Atomic Energy Agency, Vienna, 1963), Vol. II, p. 37.

[34]S. Rodriguez (private communication).